

# Regime change detection in irregularly sampled time series

Norbert Marwan, Deniz Eroglu, Ibrahim Ozken, Thomas Stemler, Karl-Heinz Wyrwoll, Jürgen Kurths

**Abstract** Irregular sampling is a common problem in palaeoclimate studies. We propose a method that provides regularly sampled time series and at the same time a difference filtering of the data. The differences between successive time instances are derived by a transformation costs procedure. A subsequent recurrence analysis is used to investigate regime transitions. This approach is applied on speleothem based palaeoclimate proxy data from the Indonesian-Australian monsoon region. We can clearly identify Heinrich events in the palaeoclimate as characteristic changes in the dynamics.

---

Norbert Marwan  
Potsdam Institute for Climate Impact Research (PIK), 14473 Potsdam, Germany,  
e-mail: marwan@pik-potsdam.de

Deniz Eroglu  
Instituto de Ciências Matemáticas e Computação, Universidade de São Paulo, Brazil  
Department of Mathematics, Imperial College London, United Kingdom  
e-mail: deniz.eroglu@imperial.ac.uk

Ibrahim Ozken  
Department of Physics, Ege University, 35100 Izmir, Turkey

Thomas Stemler  
School of Mathematics and Statistics, The University of Western Australia, Crawley, Western Australia 6009, Australia

Karl-Heinz Wyrwoll,  
School of Earth and Environment, The University of Western Australia, Crawley, Western Australia 6009, Australia

Jürgen Kurths,  
Potsdam Institute for Climate Impact Research (PIK), 14473 Potsdam, Germany  
Institute of Applied Physics of the Russian Academy of Sciences, 46 Ulyanova St., Nizhny Novgorod 603950, Russia.

## Introduction

In the last decades, palaeoclimate research has experienced an exciting progress with ever-higher resolution and better age control high-resolution records, innovative technologies and types of proxies, as well as new data series analysis approaches, such as speleothem based proxies, fluid inclusion analysis and laser ablation techniques, complex network based data analysis, etc. [1–5]. This progress helps greatly to increase our understanding of past climate variation and the mechanisms behind the climate system, but also to assess future climate-related vulnerability of our society. Of particular interest are critical transitions, such as tipping points or regime shifts, because they can bring the climate system into another mode of operation [6, 7]. Identifying tipping points from measurements is no simple task. Several approaches have been proposed, such as testing for slowing down and increase of the auto-correlation [8], reconstructing potentials of the dynamics by using the modality of the data distribution [9], using a modified detrended fluctuation analysis (DFA) [10], or the concept of stochastic resonance [11]. While dynamical transitions are rather obvious when they appear in the first two moments (i.e., in mean or variance), they can be hidden when superimposed by signals of different time scales or by noise, issues frequently observed in palaeoclimate time series. For such problems, the application of methods from nonlinear time series analysis is a well accepted perspective, e.g., by using the fluctuation of similarity (FLUS) [12]. Another promising tool for the identification of subtle transitions is the framework of recurrence plots [13]. Recurrence plots and their quantification consider the evolution of neighbouring states in a phase space. Besides characterizing different classes of dynamics or testing for synchronization and nonlinear interrelationships and couplings of multiple systems, it allows to test for dynamical regime changes with respect to different properties, such as changes in the geometry of the attractor, in the predictability of states, or in the intermittency behaviour [13–15]. The recurrence plot framework has been successfully applied to investigate past transitions, e.g., in the Asian monsoon system [16] and in the East African climate [17], and to uncover a seesaw effect within the East Asian and Indonesian-Australian summer monsoon system [18].

However, most palaeoclimate proxy records (independent of the actual archive) come with the challenge of irregular sampling. While sampling in the field or in the lab is often done on a regular depth/length axis, varying sedimentation or growth rates result in variable time-depth relationships and in time series with non-equidistant sampling points in the time-domain [19]. The most common procedure is data pre-processing using linear interpolation. However, interpolation can lead to a positive bias in autocorrelation estimation (and, thus, an overestimation of the persistence time) and a negative bias in cross correlation analysis [20]. Therefore, several approaches have been suggested for analyzing irregularly sampled time series [20–24].

In the following we will focus on a recently proposed technique that is based on a measure that compares spike trains by quantifying the effort it needs to transform one spike train to the other one [25, 26]. This measure corresponds to a modified

difference filter (a common practice to remove low-frequency variation and trends), where we determine the differences by a criterion of how close subsequent short segments of an unevenly sampled time series are by determining the cost needed to transform one segment into the following one [24]. Such comparison of successive segments has some similarity with the FLUS method [12], but instead uses the transformation cost as the similarity measure, and is thus directly applicable on irregularly sampled time series. We illustrate this approach by analyzing a speleothem-based palaeoclimate record with respect to regime transitions.

## Methods

### *Transformation costs time series (TACTS)*

Cumulative trends or low-frequency variations are common in palaeoclimate proxy records, but are often undesirable and can cause difficulties in the analysis. One frequently used solution is the difference filter, where the values of the proxy record are replaced by the differences of subsequent values,  $y(t - \Delta t/2) = x(t) - x(t - \Delta t)$ , with  $\Delta t$  the sampling time of a regularly sampled time series. Another, even more challenging problem is the irregular sampling frequently occurring in palaeoclimate proxy records. The *transformation costs time series* (TACTS) approach tries to overcome both problems by transforming irregularly sampled time series to regular ones and simultaneously using the transformation cost as the difference value. This procedure induces less loss of information compared to traditional interpolation procedures.

The core of the TACTS method is to measure the shortest distance (transformation cost) between two data segments by using two different processes: (i) *shifting points* in time which causes changes in the amplitude for marked data and (ii) *adding-deleting* operations. The process starts with dividing the data into small and equally sized segments. These segments can have different number of points, because the points are not equally sampled. The transformation costs between all sequence windows are then calculated by

$$p(S_a, S_b) = \underbrace{\sum_{(\alpha, \beta) \in C} \{\lambda_0 |t_a(\alpha) - t_b(\beta)| + \lambda_k |L_a(\alpha) - L_b(\beta)|\}}_{\text{shifting}} + \underbrace{\lambda_S (|I| + |J| - 2|C|)}_{\text{adding/deleting}}. \quad (1)$$

The equation states two distinct operations for two essential processes. If the operation is *shifting* then the first part of the equation involves, otherwise the *adding-deleting* operation involves as the second part. In the first part, the summation is over the pairs  $(\alpha, \beta) \in C$ , where  $C$  is the set of points that will be shifted in time and changed in amplitude.  $\alpha$  and  $\beta$  are the  $\alpha$ th event in the first segment ( $S_a$ ) and

the  $\beta$ th event in the second segment ( $S_b$ ). The amplitude of points which are  $\alpha$ th and  $\beta$ th elements of  $S_a$  and  $S_b$  are denoted by  $L_a(\alpha)$  and  $L_b(\beta)$  respectively. The data-adapted constants  $\lambda_0$  and  $\lambda_k$  are given by

$$\lambda_0 = \frac{M}{\text{total time}} \quad (2a)$$

$$\lambda_k = \frac{M-1}{\sum_i^{M-1} |x_i - x_{i+1}|}. \quad (2b)$$

where  $M$  is the total number of events, and  $x_i$  is the amplitude of  $i$ th element in the time series.

In the second part of Eq. (1),  $I$  and  $J$  are sets of indices of the events in  $S_a$  and  $S_b$ , respectively. The parameter  $\lambda_S$  is the cost of deleting or adding processes and is used as an optimization parameter. The selection of optimum  $\lambda_S$  is the following: first we calculate total cost time series for the entire range of  $\lambda_S \in [0, 4]$  with step size  $\Delta\lambda_S = 0.01$ . Then we examine frequency distributions for each cost time series. Since each cost value is independent of the others, we expect to have a normal distributed histogram and choose the optimal  $\lambda_S$  according to the best fit on normal distribution.

Eq. (1) is a metric distance function, satisfying the following three conditions:

- $p(S_a, S_b) \geq 0$  (positive)
- $p(S_a, S_b) = p(S_b, S_a)$  (symmetric)
- $p(S_a, S_c) \leq p(S_a, S_b) + p(S_b, S_c)$  (triangle inequality)

Now we illustrate the method for two consecutive segments. Irregularly sampled data is equally spaced into small windows which are given as state  $a$  ( $S_a = \{a_\alpha\}_{\alpha=1}^4$ ) and state  $b$  ( $S_b = \{b_\beta\}_{\beta=1}^3$ ). The costs computed between the states and all details are given in Fig. 1 step by step.

Note that the decision of which operation process to minimize costs is important. The transformation by shifting costs  $\lambda_0|t_a(\alpha) - t_b(\beta)| + \lambda_1|L_a(1) - L_b(1)|$  and deleting and adding a point costs  $2\lambda_S$ . Here we chose the least cost operation to either shift or delete/add. Therefore, in the algorithm, we consider all these possibilities and chose the operation carefully.

The final appearance of the cost time series is as follows: assume that we have an irregularly sampled time series  $\{u_i\}_{i=1}^N$ , where  $N$  is the number of points. The data is divided to a set of  $W$ -sized  $n$  segments and each segment has a minimum of a certain number of points, therefore,

$$TACTS = \{p(W_i, W_i + 1)\}_{i=1}^{n-1}$$

for all sequence windows. This leads to an equally sampled and detrended time series. The resulting cost values series can be considered as the difference filtered time series with a regularly sampled time axis and can be further analysed with standard or advanced time series analysis tools, e.g., in order detect regime shifts (Fig. 1).

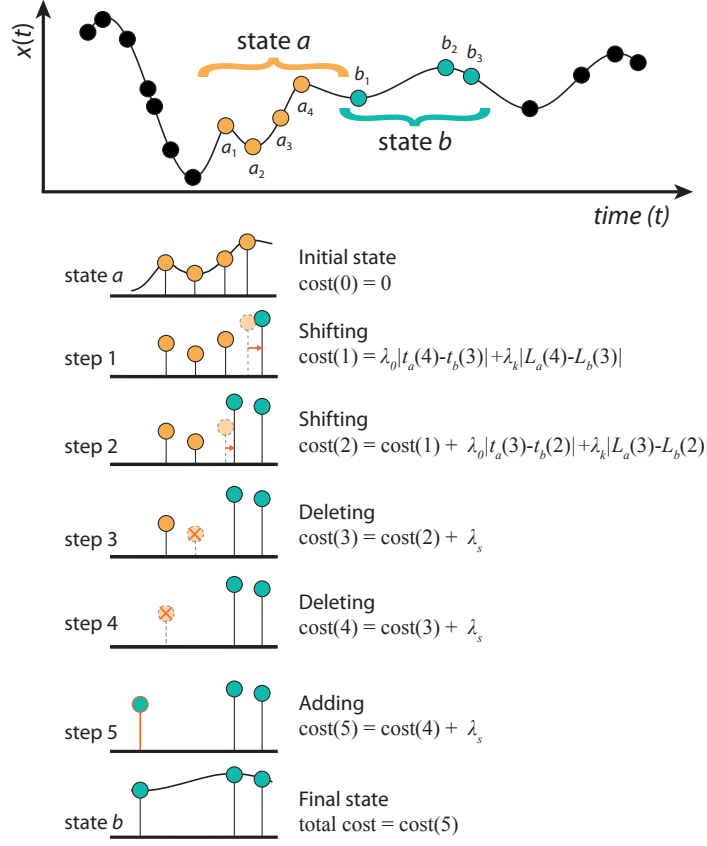


**Fig. 1** Illustration of the transformation cost time series method, which finds the minimum transformation cost between two data segments such as state  $a$  and state  $b$  in the top panel. In five steps state  $a$  is transformed into state  $b$ . At steps 1 and 2, we apply *shifting* a point in time and, as a consequence of shifting, changing the amplitude of the point. These operations cost regarding to first part of Eq. (1). Steps 3 and 4 are *deleting* and step 5 is *adding* a point; each of these operations costs a constant  $\lambda_s$ . The costs are written next to the related processes according to Eq. (1).

### Recurrence analysis

Recurrence is an ubiquitous property of many dynamical systems. Slight changes in observed recurrence behaviour allow to infer changes in the dynamics [13, 27]. In order to investigate recurrence properties, recurrence plots and recurrence quantification analysis have been developed [13, 28]. A recurrence plot is the graphical representation of those times  $j$  at which a system recurs to a previous state  $\vec{x}_i$ :

$$R_{i,j} = \Theta(\varepsilon - \|\vec{x}_i - \vec{x}_j\|), \quad i, j = 1, \dots, N \quad (3)$$

with  $\Theta$  the Heaviside function,  $\varepsilon$  a recurrence threshold,  $\|\vec{x}_i - \vec{x}_j\|$  the Euclidean distance between two states  $\vec{x}_i$  and  $\vec{x}_j$  in the phase space, and  $N$  the number of observations (or time series length). Such a recurrence plot consists of typical large-scale and small-scale features that can be used to interpret the dynamics visually. Important features are diagonal lines: similar evolving epochs of the phase space trajectory cause diagonal structures parallel to the main diagonal in the recurrence plot. The length  $l$  of such diagonal line structures depends on the dynamics of the system (periodic, chaotic, stochastic) Fig. 2 and can be directly related with dynamically invariant properties, like  $K_2$  entropy [13]. Therefore, recurrence quantification analysis (RQA) uses the features within the recurrence plots for defining measures of complexity. For example, the distribution  $P(l)$  of line lengths  $l$  is used by several measures of complexity in order to characterise the system's dynamics in terms of predictability/determinism or laminarity. The measure *determinism* DET is the fraction of recurrence points (i.e.,  $R_{i,j} = 1$ ) that form diagonal lines and can be computed by

$$DET = \frac{\sum_{l_{\min}}^N l \cdot P(l)}{\sum_{i,j=1}^N R_{i,j}}. \quad (4)$$

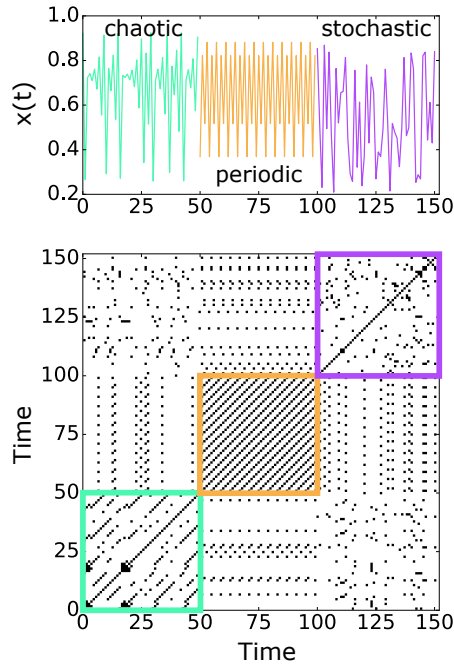


**Fig. 2** Example of a recurrence plot for changing dynamics from chaotic via periodic to stochastic dynamics, each lasting 50 time steps. In the periodic region, continuous long diagonal lines are observed, in the chaotic region, shorter diagonals and single points appear, and in the stochastic part, we find almost only single points.

In order to study the time-dependent behaviour of a system or time series, RQA measures can be computed within a moving window, applied on the time series. The window has size  $w$  and is moved with a step size  $s$  over the data in such a way that succeeding windows overlap with  $w - s$ . This technique can detect chaos-period and also more subtle chaos-chaos transitions [13], or different kinds of transitions between strange non-chaotic behaviour and period or chaos [29]. Moreover, the reliability of several RQA measures was investigated by their scaling properties with respect to critical points in the dynamics [30].

## Palaeoclimate regime transition

To illustrate the power of the techniques we advocate here, we choose as illustrating example a speleothem  $\delta^{18}\text{O}$  record from the Secret Cave at Gunung Mulu in Borneo/ Indonesia [31]. This particular record has been interpreted as a time se-

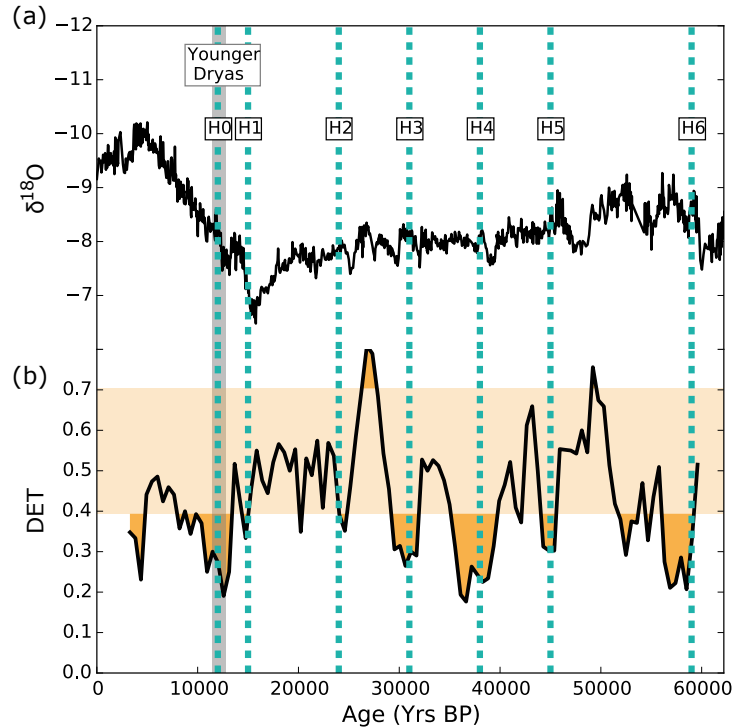


**Fig. 3** (a)  $\delta^{18}\text{O}$  record of Secret Cave, Borneo. (b) RQA-determinism  $DET$ , Eq. (4), time series resulting from the transformation cost time series. The light orange band of the  $DET$  indicates the 90% confidence interval. The vertical lines H1–H6 give the six Heinrich events as well as H0, the Younger-Dryas.

ries of the dynamics of the East Asian–Indonesian – northwest Australia monsoon. This monsoon regime provides a circulation regime that strongly links both hemispheres and serves as a major heat source, playing a significant role at planetary scale [32, 33]. Central to its geography is the Maritime Continent which provides a core region of monsoon activity [34, 35]. A transect in regional precipitation patterns from the northern part of the Maritime Continent to the northern margin of Australia coincides with a change from the dominance of the boreal summer monsoon to the austral summer monsoon [33, 35, 36]. The transect captures key palaeoproxy monsoon records and has the potential to provide details of the function of the monsoon regime over Quaternary time scales [31, 37–39]. Imbedded in some of these records are short-lived millennial and centennial scale events, and, more general, relatively short-lived phases of climate instability.

While the full proxy record is around 100,000 years, we only analyze the last 62,000 years of the  $\delta^{18}\text{O}$  record (Fig. 3(a)). Before the 62,000 years many gaps appear and the data become too sparse to give any useful information about. The record used for the analysis contains about 1,200 data points. Time intervals between measurements are irregular and follow a Gamma distribution with a skewness of 4.9. In our analysis we use a window length of  $\approx 210$  years to calculate the TACTS. While the parameters  $\lambda_{0,k}$  are determined by Eq. (2), we optimize  $\lambda_S = 1.07$ .

The next step is to analyze the regularly sampled TACTS with RQA using a sliding window method. We consider 30 data points (or 6,200 years) of the TACTS as our window size. Given the average number of points in the proxy record, 30 data points of the TACTS correspond to approximately 100 to 140 points in the original proxy. Using an overlap of 90% of consecutive windows, we determine the *DET* (Eq. (4)) for each window with length of 6,200 years (Fig. 3(b)). The recurrence threshold is selected to be  $\varepsilon = 20\%$  of the standard deviation of the data in the particular window. The advantage of this  $\varepsilon$  selection scheme is that it allows us to analyze proxy records with inherent non-stationarity. In addition, we determine the statistical significance of *DET* using the bootstrapping method as outlined in [16] (light red band in Fig. 3(b)).

The determinism *DET* indicates several distinct regime changes in the time series from less to more predictable (and vice versa) dynamics (Fig. 3(b)). Most minima of *DET*, signified as periods of decreased predictability, coincide with the so called Heinrich events (H1 to H6). Heinrich events are identified in the North Atlantic sediments as layers of ice-rafted debris, associated with the coldest phase just before the Dansgaard-Oeschger Events, and result from episodic discharge of icebergs in the Hudson Bay region [40, 41].

Heinrich events are well represented in the Chinese speleothem and loess record as periods of weakened summer monsoon and intensified winter monsoon. [42]. In their interactions with the Siberian Mongolian High of the East Asian Winter Monsoon they can be expected to trigger cold surges which leave their imprint in the proxy palaeoclimate record [43]. During the East-Asian Winter Monsoon (EAWM), the Siberian High with its central pressure reaching in excess of 1035 hPa, dominates much of the Eurasian continent. Strong northwesterly flows occur at its eastern margins, where one branch of the flow separates and first is directed east-



ward into the subtropical western Pacific and then tends southward in the direction of the South China Sea. These cold air ‘excursions’, also described as ‘cold surges’, are channeled by the trough southwards and are a characteristic feature of the EAWM [44]. Their path is in part related to relief controls of the Tibetan Plateau. Cold surges transport absolute vorticity and water vapour up-stream of the South China Sea to the Equator [45] and lead to the flare-up of convective activity over the Maritime Continent [46]. In the Borneo region, cold surges enhance surface cyclonic circulation triggering the Borneo Vortex, which leads to deep convection giving rise to heavy rainfall events [45, 47].

It is noteworthy that in raw  $\delta^{18}\text{O}$  record from the Secret Cave the Heinrich events are almost indistinguishable from other variations in the time series. In the original work by Carolin *et al.*, H1 to H6 were detected by visual comparison of the record to others (e.g., NGRIP), but the Younger Dryas (coinciding with the H0 event), was not detected [31]. However, our method clearly extracts these events, including the previously not detected Younger Dryas, and highlights the hidden impact of such distal forcing. Moreover, it allows an objective, quantitative analysis, while Carolin *et al.* rely on the subjective method of matching extreme proxy values with specific dates. At present, the Borneo Vortex leaves a strong climate signal on the regional precipitation patterns [47]. We propose that the prominence of the ‘instability climate phases’, coincident with the timing of Heinrich events in the Borneo record, is an expression of regional controls that are linked to the operation of the Borneo Vortex. The claim draws attention to the need to give more consideration to specific regional controls in explaining the palaeoclimate proxy record rather than simply appeal to global or hemispheric controls.

## Conclusion

We have used the Secret Cave  $\delta^{18}\text{O}$  record from Borneo to illustrate the usefulness of the novel TACTS method for analyzing palaeoclimate records. TACTS can transform irregularly sampled time series into a regularly sampled cost time series. This is an important step, since most modern time series analysis methods – like the RQA used here – require a regular sampled time series as an input. Furthermore, the TACTS method is less biased than interpolation methods frequently used to transform irregularly sampled into regularly sampled data sets. This transformation only requires three parameters. The two parameters  $\lambda_{0,k}$  are given by the average amplitude and frequency of the record (see Eq. (2)), while  $\lambda_S$  needs to be optimized. Being a difference filter, the TACTS method lends itself naturally for palaeoclimate investigations, where proxy records often have some non-stationarity and usually need to be detrended. As we have shown the detrending is build into the TACTS method, therefore we do not need this additional step in our time series analysis.

Applying the TACTS and RQA approach on palaeoclimate data from the Secret Cave speleothem, we were able to identify regime changes in the monsoon activity during the last 62,000 years. We report on several distinct regime changes coinciding

with the Heinrich events H1 to H6 and therefore add quantitative evidence of these impacts to previous, more qualitative studies [31]. Moreover, our analysis clearly unveils that also the Younger Dryas had an impact on the monsoon activity over the Maritime Continent.

Given that irregular sampling of proxy records is quite common in Earth science, the TACTS method has large potential in quantitative Earth science without prior modification or preprocessing the data.

**Acknowledgements** This work was supported by grants from the Leibniz Association, grant SAW-2013- IZW-2 (Gradual environmental change versus single catastrophe – Identifying drivers of mammalian evolution) and the European Union’s Horizon 2020 Research and Innovation programme under the Marie Skłodowska-Curie grant agreement No 691037 (RISE project QUantitative palaeoEnvironments from SpeleoThems QUEST). We thank Sebastian Breitenbach for fruitful discussions and support.

## References

1. P. Dennis, P. Rowe, T. Atkinson, *Geochimica et Cosmochimica Acta* **65**(6), 871 (2001). DOI 10.1016/S0016-7037(00)00576-7
2. F. McDermott, *Science* **294**(5545), 1328 (2001). DOI 10.1126/science.1063678
3. D.J. Kennett, S.F.M. Breitenbach, V.V. Aquino, Y. Asmerom, J. Awe, J.U.L. Baldini, P. Bartlein, B.J. Culleton, C. Ebert, C. Jazwa, M.J. Macri, N. Marwan, V. Polyak, K.M. Pruffer, H.E. Ridley, H. Sodemann, B. Winterhalder, G.H. Haug, *Science* **338**(6108), 788 (2012). DOI 10.1126/science.1226299
4. K. Rehfeld, N. Marwan, S.F.M. Breitenbach, J. Kurths, *Climate Dynamics* **41**(1), 3 (2013). DOI 10.1007/s00382-012-1448-3
5. F.H. McRobie, T. Stemler, K.H. Wyrwoll, *Quaternary Science Reviews* **121**, 120 (2015). DOI 10.1016/j.quascirev.2015.05.011. URL <http://dx.doi.org/10.1016/j.quascirev.2015.05.011>
6. T.M. Lenton, H. Held, E. Kriegler, J.W. Hall, W. Lucht, S. Rahmstorf, H.J. Schellnhuber, *Proceedings of the National Academy of Sciences* **105**(6), 1786 (2008). DOI 10.1073/pnas.0705414105
7. M. Scheffer, S.R. Carpenter, T.M. Lenton, J. Bascompte, W. Brock, V. Dakos, J. van de Koppel, I.A. van de Leemput, S.A. Levin, E.H. van Nes, M. Pascual, J. Vandermeer, *Science (New York, N.Y.)* **338**(6105), 344 (2012). DOI 10.1126/science.1225244
8. M. Scheffer, J. Bascompte, W.A. Brock, V. Brovkin, S.R. Carpenter, V. Dakos, H. Held, E.H. van Nes, M. Rietkerk, G. Sugihara, *Nature* **461**(7260), 53 (2009). DOI 10.1038/nature08227
9. V.N. Livina, F. Kwasniok, T.M. Lenton, *Climate of the Past* **6**(1), 77 (2010). DOI 10.5194/cp-6-77-2010
10. V.N. Livina, T.M. Lenton, *Geophysical Research Letters* **34**(3), L03712 (2007). DOI 10.1029/2006GL028672
11. H. Braun, P. Ditlevsen, J. Kurths, M. Mudelsee, *Paleoceanography* **26**(3), PA3214 (2011). DOI 10.1029/2011PA002140
12. N. Malik, Y. Zou, N. Marwan, J. Kurths, *EPL (Europhysics Letters)* **97**(4), 40009 (2012). DOI 10.1209/0295-5075/97/40009
13. N. Marwan, M.C. Romano, M. Thiel, J. Kurths, *Physics Reports* **438**(5–6), 237 (2007). DOI 10.1016/j.physrep.2006.11.001
14. R.V. Donner, J. Heitzig, J.F. Donges, Y. Zou, N. Marwan, J. Kurths, *European Physical Journal B* **84**, 653 (2011). DOI 10.1140/epjb/e2011-10899-1

15. D. Eroglu, N. Marwan, S. Prasad, J. Kurths, *Nonlinear Processes in Geophysics* **21**, 1085 (2014). DOI 10.5194/npg-21-1085-2014
16. N. Marwan, S. Schinkel, J. Kurths, *Europhysics Letters* **101**, 20007 (2013). DOI 10.1209/0295-5075/101/20007
17. J.F. Donges, R.V. Donner, M.H. Trauth, N. Marwan, H.J. Schellnhuber, J. Kurths, *Proceedings of the National Academy of Sciences* **108**(51), 20422 (2011). DOI 10.1073/pnas.1117052108
18. D. Eroglu, F.H. McRobie, I. Ozken, T. Stemler, K.H. Wyrwoll, S.F.M. Breitenbach, N. Marwan, J. Kurths, *Nature Communications* **7**, 12929 (2016). DOI 10.1038/ncomms12929
19. S.F.M. Breitenbach, K. Rehfeld, B. Goswami, J.U.L. Baldini, H.E. Ridley, D.J. Kennett, K.M. Prufer, V.V. Aquino, Y. Asmerom, V.J. Polyak, H. Cheng, J. Kurths, N. Marwan, *Climate of the Past* **8**(5), 1765 (2012). DOI 10.5194/cp-8-1765-2012
20. K. Rehfeld, N. Marwan, J. Heitzig, J. Kurths, *Nonlinear Processes in Geophysics* **18**(3), 389 (2011). DOI 10.5194/npg-18-389-2011
21. J.D. Scargle, *The Astrophysical Journal* **263**, 835 (1982). DOI 10.1086/160554
22. P. Stoica, N. Sandgren, *Digital Signal Processing* **16**(6), 712 (2006). DOI 10.1016/j.dsp.2006.08.012
23. K. Rehfeld, J. Kurths, *Climate of the Past* **10**(1), 107 (2014). DOI 10.5194/cp-10-107-2014
24. I. Ozken, D. Eroglu, T. Stemler, N. Marwan, G.B. Bagci, J. Kurths, *Physical Review E* **91**(6), 062911 (2015). DOI 10.1103/PhysRevE.91.062911
25. J.D. Victor, K.P. Purpura, *Network: Computation in Neural Systems* **8**(2), 127 (1997). DOI 10.1088/0954-898X/8/2/\_003
26. Y. Hirata, K. Aihara, *Journal of Neuroscience Methods* **183**(2), 277 (2009). DOI 10.1016/j.jneumeth.2009.06.030
27. N. Marwan, *International Journal of Bifurcation and Chaos* **21**(4), 1003 (2011). DOI 10.1142/S0218127411029008
28. N. Marwan, *European Physical Journal – Special Topics* **164**(1), 3 (2008). DOI 10.1140/epjst/e2008-00829-1
29. E.J. Ngamga, A. Nandi, R. Ramaswamy, M.C. Romano, M. Thiel, J. Kurths, *Physical Review E* **75**(3), 036222 (2007). DOI 10.1103/PhysRevE.75.036222
30. O. Afsar, D. Eroglu, N. Marwan, J. Kurths, *EPL (Europhysics Letters)* **112**(1), 10005 (2015)
31. S.a. Carolin, K.M. Cobb, J.F. Adkins, B. Clark, J.L. Conroy, S. Lejau, J. Malang, A.a. Tuen, *Science (New York, N.Y.)* **340**(2013), 1564 (2013). DOI 10.1126/science.1233797
32. J.L. McBride, in *Monsoon Meteorology*, ed. by C.P. Chang, T.N. Krishnamurti (Oxford University Press, Oxford, U.K., 1987), pp. 203–231
33. C.P. Chang, Z. Wang, H. Hendon, in *The Asian Monsoon*, Springer Praxis Books (Springer Berlin Heidelberg, 2006), pp. 89–127
34. C.S. Ramage, *Monthly Weather Review* **96**(6), 365 (1968)
35. C.P. Chang, P. Harr, J. McBride, H.H. Hsu, in *East Asian Monsoon. World Scientific Series on Meteorology of East Asia, vol. 2*, ed. by C.P. Chang (World Scientific Publishing Co. Pte. Ltd, Singapore, 2004), pp. 107–150
36. A. Robertson, V. Moron, J.H. Qiam, C.P. Chang, F. Tangan, E. Aldrian, T. Koh, L. Jueng, in *The global monsoon system: research and forecast*, ed. by C.P. Chang, Y. Ding, N.C. Lau, R. Johnson, B. Eang, T. Yasunari (World Scientific, 2011), pp. 85–109
37. L.K. Ayliffe, M.K. Gagan, J.x. Zhao, R.N. Drysdale, J.C. Hellstrom, W.S. Hantoro, M.L. Griffiths, H. Scott-Gagan, E. St Pierre, J.a. Cowley, B.W. Suwargadi, *Nature communications* **4**(May), 2908 (2013). DOI 10.1038/ncomms3908
38. R.F. Denniston, K.H. Wyrwoll, V.J. Polyak, J.R. Brown, Y. Asmerom, A.D.W. Jr., Z. LaPointe, R. Ellerbroek, M. Barthelmes, D. Cleary, J. Cugley, D. Woods, W.F. Humphreys, *Quaternary Science Reviews* **78**(0), 155 (2013). DOI <http://dx.doi.org/10.1016/j.quascirev.2013.08.004>
39. J.W. Partin, K.M. Cobb, J.F. Adkins, B. Clark, D.P. Fernandez, *Nature* **449**(7161), 452 (2007). DOI 10.1038/nature08125
40. A.C. Clement, L.C. Peterson, *Reviews of Geophysics* **46**(2006), 1 (2008). DOI 10.1029/2006RG000204
41. D. McNeill, P.R. Halloran, P. Good, R.A. Betts, *Wiley Interdisciplinary Reviews: Climate Change* **2**(5), 663 (2011). DOI 10.1002/wcc.130

42. Z. An (ed.), *Late Cenozoic Climate Change in Asia, Developments in Paleoenvironmental Research*, vol. 16 (Springer Netherlands, Dordrecht, 2014). DOI 10.1007/978-94-007-7817-7
43. K.H. Wyrwoll, J. Wei, Z. Lin, Y. Shao, F. He, *Quaternary Science Reviews* **149**, 102 (2016). DOI 10.1016/j.quascirev.2016.04.015
44. K.M. Lau, C.P. Chang, in *Monsoon Meteorology* (Oxford University Press, 1987), pp. 161–202
45. S. Koseki, T.Y. Koh, C.K. Teo, Q. J. R. Meteorol. Soc. **139**(675), 1566 (2013). DOI 10.1002/qj.2052
46. J.C.L. Chan, C.Y. Li, in *East Asian Monsoon, World Scientific Series on Asia-Pacific Weather and Climate*, vol. 2, ed. by C.P. Chang (World Scientific, 2004), pp. 54–106
47. S.H. Ooi, A.A. Samah, P. Braesicke, *Journal of Geophysical Research Atmospheres* **116**(21) (2011). DOI 10.1029/2011JD015991